Research Article

Journal of RAMAN SPECTROSCOPY

Received: 19 March 2009 Accepted: 14 April 2009 Published online in Wiley Interscience: 2 June 2009

(www.interscience.wiley.com) DOI 10.1002/jrs.2344

Direct visual evidence for chemical mechanisms of SERRS via charge transfer in Au_{20}–pyrazine–Au_{20} junction

Mengtao Sun,[a]* Zhipeng Li,[a] Yajun Liu[b] and Hongxing Xu[a,c]

The essence of the chemical mechanism for surface-enhanced resonance Raman scattering (SERRS) is the charge transfer (CT) between the metal and the molecule at the resonant electronic transition, which results in the mode-selective enhancement in the SERRS spectrum. The site-orientated CT can directly interpret the mode-selective chemical enhancement in SERRS. However, it is a great challenge to intutively visualize the orientation and site of the CT. In this paper, for the pyrazine–Au_2 complex, a three-dimensional (3D) cubic representation is built to provide direct visual evidence for chemical mechanisms of SERRS via CT from the Au_2 cluster to pyrazine at the resonant electronic transition. The relationship between the mode-selective enhancements in SERRS and the site-orientated CT was clearly revealed. The intracluster excitation (analog of plasmon excitation in large naonoparticles) was also visualized by the 3D cubic presentation, which provided the direct evidence of local electromagnetic field enhancement of SERRS. To study the quantum size effect and the coupling effect of the nanoparticles, the photoexcitation mechanisms of the Au_{20}–pyrazine complex and the Au_{20}–pyrazine–Au_{20} junction were also investigated. The tunneling charge transfer from one Au_{20} cluster to another Au_{20} cluster outside the pyrazine in Au_{20}–pyrazine–Au_{20} junction was also revealed visually. The calculated normalized extinction spectra of Au nanoparticles using the generalized Mie theory reveal that the resonance peak is red-shifted due to the coupling between particles.

Keywords: chemical mechanisms; SERRS; charge transfer; Au_{20}–pyrazine–Au_{20} junction

Introduction

Since the discovery of surface-enhanced Raman scattering (SERS) and surface enhanced-resonance Raman scattering (SERRS), two primary enhancing mechanisms have been presented.[1–10] One is the electromagnetic (EM) mechanism,[4–6] which is caused by the strong surface plasmon resonance of the rough metal surface coupled to the incident light. EM enhancement should be a nonselective amplification mechanism for Raman scattering by all molecules adsorbed on a particular surface. When the coupling effect of the nanoparticles is considered, the EM enhancement of SERS can be up to the order of 10^{10}.[6] The other enhancement mechanism is chemical a mechanism via charge transfer (CT) between the metal and the molecule at resonant electronic transition.[7–11] When the molecule chemically adsorbs on the metal forming chemical bonds with the active sites (adatoms) of the surface and the exciting line is in resonance with the CT band of the molecule–surface adduct, selective chemical enhancement can occur. When the coupling effect of the nanoparticles is considered, the chemical enhancement of SERRS can be up to the order of 10^6.[2] For a clear understanding of the chemical enhancement mechanism for SERRS, the most convenient way is to visualize the orientation and site of CT at the resonant electronic transition. Site-orientated CT can directly interpret the mode-selective chemical enhancement in SERRS.

It is a great challenge to distinguish chemical enhancement from the EM mechanism through a visual theoretical method. The charge difference density in the three-dimensional (3D) cubic representation can be the best candidate for visualization,[11–15] which can reveal visually photo-induced CT from the metal to the molecule or intracluster excitation at resonant electronic transitions.[11] We have theoretically investigated the enhancement mechanism on the SERS of pyridine adsorbed on the Ag nanoparticles[14,15] with quantum chemical theory, generalized Mie theory, and 3D finite-difference time domain (3D-FDTD) method, where the effects of quantum size and binding site on SERS have been clearly shown and regions of EM and chemical enhancements from 300 to 1000 nm have been successfully clarified with charge difference density. We also investigated the chemical enhancement mechanism (CT) on the SERS in the metal–para-aminothiophenol (PATP)–metal junction with the quantum chemical method, in which the tunneling CT at incident light of 1064 nm has been visualized with charge difference density.[12]

In this paper, the direct theoretical evidence for the chemical mechanism of SERRS via CT between the molecule and the metal cluster is provided in visual way using charge difference density. The relationship between the selective chemical enhancements of the SERRS spectrum and the resonant CT transition is revealed visually, as well as the intracluster excitation, which is evidence for the local EM enhancement.

* *Correspondence to: Mengtao Sun, Beijing National Laboratory for Condensed Matter Physics, Institute of Physics, Chinese Academy of Sciences, P. O. Box 603-146, Beijing, 100190, China. E-mail: mtsun@aphy.iphy.ac.cn*

a *Beijing National Laboratory for Condensed Matter Physics, Institute of Physics, Chinese Academy of Sciences, P. O. Box 603-146, Beijing, 100190, China*

b *College of Chemistry, Beijing Normal University, Beijing, 100875, China*

c *Division of Solid State Physics, Lund University, Lund 21100, Sweden*

Journal of RAMAN SPECTROSCOPY

Method

All the quantum chemical calculations were performed using the Gaussian 03 suite software.[16] The geometry of pyrazine (Fig. 1(a)) was optimized by density functional theory (DFT)[17] with the B3PW91 functional.[18] The normal Raman scattering (NRS) spectrum of pyrazine was calculated by the DFT B3PW91 method. The absorption spectrum of pyrazine was calculated using the time-dependent DFT (TD-DFT)[19] B3PW91 method. The 6-31G basis set was employed in all the above calculations.

The pyrazine–Au_2 complex (Fig. 1(b)) was chosen as the calculation model for both theoretical and experimental reasons. Theoretically, because of the high computational demands for large clusters, most electronic structural studies had to adopt small silver clusters to mimic the model surface.[8,11] Experimentally, Peyser-Capadona *et al*.[20] have shown that small (2–8 atoms) silver clusters encapsulated in a dendrimer or peptide scaffold can produce single-molecule Raman scattering characteristic of the scaffold. The pyrazine–Au_2 complex was optimized by the DFT B3PW91 method in conjunction with the LanL2dz basis set.[21] Its NRS spectrum and the preresonance Raman spectrum near the CT resonance transition were calculated at the same calculation level of B3PW91/LanL2dz. The optical absorption spectrum of the pyrazine–Au_2 complex was calculated at the TD-B3PW91/LanL2dz calculation level at the B3PW91/LanL2dz optimized ground-state geometry (hereafter denoted as TD-B3PW91/LanL2dz//B3PW91/LanL2dz). At the electronic resonant excitation, the CT between the molecule and metal and intracluster (electron–hole pairs) excitation was identified with charge difference density.

To study the influence of the quantum size effect and the coupling effect of the nanoparticles on SERRS, the pyrazine–Au_{20} complex and the Au_{20}–pyrazine–Au_{20} junction (Figs 1(c) and (d)) were optimized and their NRS spectra were calculated at the B3PW91/LanL2dz calculation level. Their optical absorption spectra were calculated at the TD-B3PW91/LanL2dz//B3PW91/LanL2dz calculation level. The intracluster excitation and CT from the Au_{20} cluster to pyrazine on resonant electronic transitions were visualized with charge difference density.

To study the influence of the coupling effect of nanoparticles on the excinction spectra, the normalized extinction spectra of Au nanoparticles were calculated by the general Mie theory[22] with the multipole taken as 30 to ensure convergence. The diameter of the nanoparticle is 50 nm. The separations of the dimer are 1 and 2 nm for the red and blue curves, respectively. For a single Au particle, the dipolar resonance peak is at about 510 nm. Owing to the coupling between particles, the resonance peak is red-shifted to 580 nm for the dimer with a separation 1 nm.

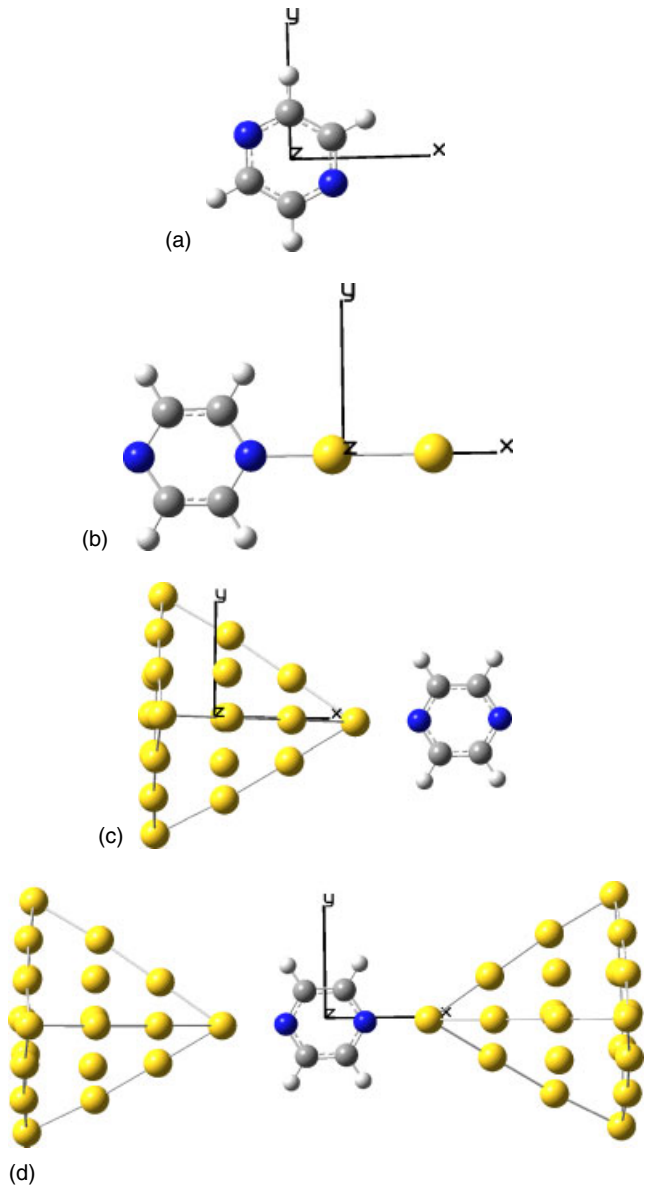

Figure 1. Chemical structures of (a) pyrazine, (b) pyrazine–Au_2, (c) pyrazine–Au_{20} complex, and (d) Au_{20}–pyrazine–Au_{20} junction.

Results and Discussion

Static chemical enhancement mechanism and normal Raman scattering spectra

For the pyrazine–Au_2 complex, because of the interaction between Au_2 and pyrazine, the 0.11 electron transfer from pyrazine to Au_2 results in a 10-times increase of the static permanent polarizability compared to isolated pyrazine, as shown in Table 1. So, the NRS spectrum of the pyrazine–Au_2 complex was enhanced by the static chemical enhancement (NRS spectrum is enhanced by the CT between pyrazine and Au_2 at the ground state),[8] and the enhancement is less than 10^1 compared to the NRS spectrum of isolated pyrazine (Fig. 2). In the NRS spectrum of isolated pyrazine, there are three strong Raman peaks: ring breathing, C–H bending, and ring stretching normal modes (Fig. 2(a)). Owing to the interaction between the Au_2 cluster and pyrazine, the

Table 1. The B3PW91-calculated static polarizabilities (in a.u.) of pyrazine, pyrazine–Au_2, pyrazine–Au_{20} complex, and Au_{20}–pyrazine–Au_{20} junction at the ground states. Their Cartesian coordinates are shown in Fig. 1

	xx	yy	zz
Pyrazine	56.535	62.196	19.099
Pyrazine–Au_2	194.297	109.007	77.351
Pyrazine–Au_{20} complex	934.998	805.875	769.438
Au_{20}–Pyrazine–Au_{20} junction	2186.298	1521.281	1488.307

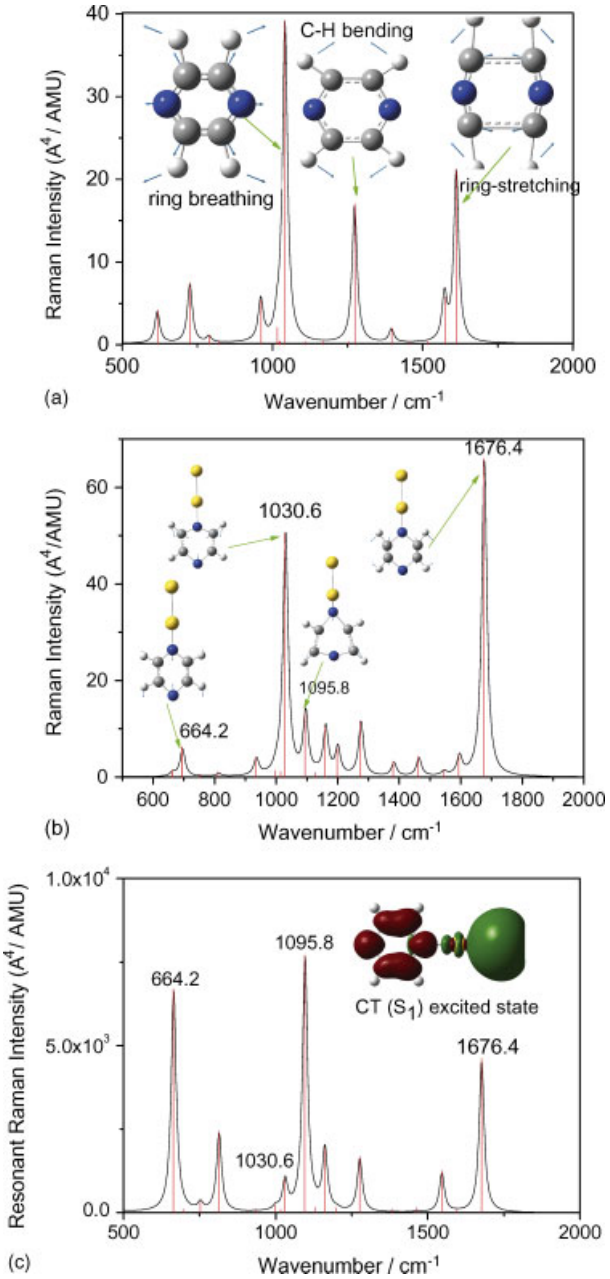

Figure 2. NRS spectra of (a) pyrazine, (b) pyrazine–Au_2 complex, and (c) SERRS spectrum of pyrazine–Au_2 complex, where the incident light resonates with CT (S_1) excited state, see the inset in Fig. 2 (c).

ring breathing mode (1009 cm^{-1}) of pyrazine splits into two ring deformation modes: one mode (1030.8 cm^{-1}) involves the motion of N when near the Au_2 cluster; the other one (1095.6 cm^{-1}) involves the motion of N when far from the Au_2 cluster (Fig. 2(b)). For the NRS spectrum of the pyrazine–Au_2 complex, the ring deformation mode (1030.8 cm^{-1}) and the ring stretching modes were strongly enhanced. The C–H bending normal mode is not strongly enhanced since its motion is perpendicular to the Au–N bonds.

Chemical enhancement mechanism and SERRS spectrum

The lowest 6 singlet excited states of pyrazine and the lowest 10 singlet excited states of the pyrazine–Au_2 complex were calculated (Table 2). Owing to the interaction between pyrazine and Au_2, some new CT excited states occur (Fig. 3), and the first excited state of the pyrazine–Au_2 complex is red-shifted to 389 nm, compared to that of the isolated pyrazine at 328 nm.

Table 2. The TD-B3PW91//B3PW91-calculated electronic excitation energies (nm) and oscillator strengths (*f*) for pyrazine and the pyrazine–Au_2 complex

	Pyrazine		Pyrazine–Au_2	
	nm	*f*	nm	*f*
S_1	328.06	0.0081	388.80	0.0009
S_2	283.98	0.0000	359.12	0.2040
S_3	231.15	0.0000	347.85	0.0000
S_4	220.07	0.0652	347.84	0.0000
S_5	205.42	0.0000	322.47	0.0024
S_6	180.27	0.0526	320.84	0.0024
S_7			309.45	0.0003
S_8			309.39	0.0000
S_9			306.67	0.0059
S_{10}			299.39	0.0000

Since S_1 of the pyrazine–Au_2 complex is the CT excited state (where the holes and electrons are localized on the Au_2 cluster and pyrazine, respectively, see Fig. 3), the Raman signal should be strongly enhanced by chemical mechanism when the incident light has energy near that of this excited state. The profile of the SERRS spectrum should be different from that of the NRS spectrum because of the selective chemical enhancement. To confirm this, we calculated the SERRS spectrum of the pyrazine–Au_2 complex (Fig. 2(c)), and compared it with the NRS spectrum. The profile of the preresonance Raman spectrum at the first CT excited state (S_1) is significantly different from the NRS spectrum, and the enhancement is of the order of 10^1–10^3 for different normal modes (detailed analysis can be seen from the next paragraph), which is the spectral evidence (mode selective) for chemical enhancement. So, the spectral profile evidence is consistent with the visual CT evidence, which provides the evidence for chemical enhancement simultaneously.

We now interpret the relationship between the SERRS spectrum and the CT from the Au_2 cluster to pyrazine at the resonant electronic transition. The electrons transfer from the Au_2 cluster to two N atoms, four C atoms, and two C=C bonds at the S_1 resonant transition (Fig. 3). For the normal mode of the ring stretching mode (664.2 cm^{-1}), motions of the two N atoms along the Au–N bond are involved, so the Raman intensities of this vibrational mode in SERRS is strongly enhanced (8×10^3). For the ring deformation mode (1030.8 cm^{-1}), the Raman intensity of the NRS was strongly enhanced, but the ring deformation mode (1093.2 cm^{-1}) was not strongly enhanced. For SERRS, the Raman intensity of the ring deformation modes (1030.8 cm^{-1}) was not strongly enhanced (1.8×10^1), while the ring deformation mode (1093.2 cm^{-1}) was strongly enhanced (6.0×10^2), compared to the NRS spectrum of the pyrazine–Au_2 complex. The reason is that the motion of the N atom in the ring deformation mode (1093.2 cm^{-1}) is close to the Au_2 cluster, which is easily and strongly influenced by the CT on the resonant electronic transition, but the motion of N atom for the ring deformation mode (1030.8 cm^{-1}) is far from the Au_2 cluster, which is weakly influenced by the CT, compared to the ring deformation mode (1093.2 cm^{-1}). For the ring stretching normal modes (1676.4 cm^{-1}), the motions of the C=C stretching mode

Journal of RAMAN SPECTROSCOPY

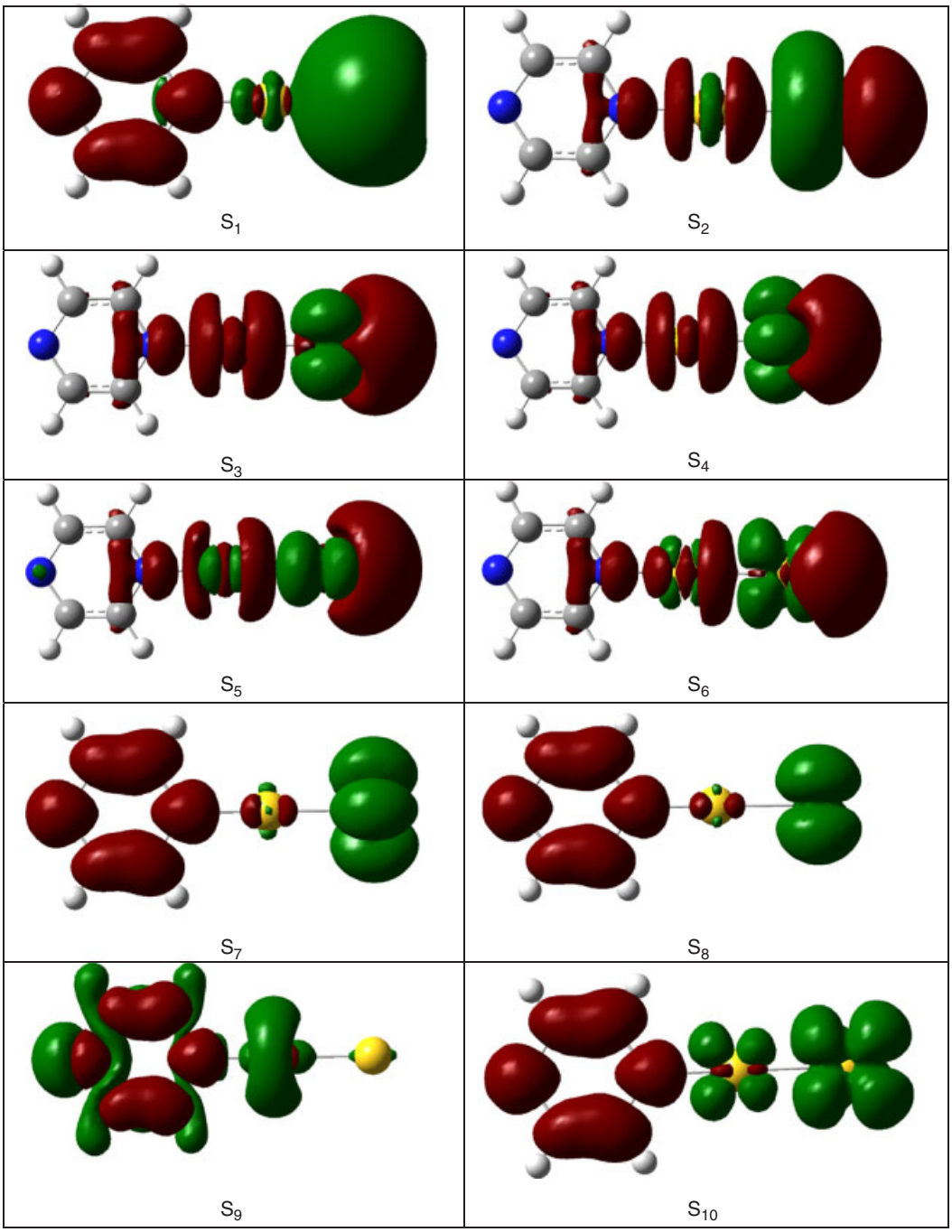

Figure 3. Charge difference densities for the lowest 10 singlet excited states in the pyrazine–Au_2 complex, where the green and red stand for hole and electron, respectively.

along the Au–N bond are strongly involved, and the transferred electrons are mainly localized on the four C atoms and the C═C bond, so the Raman intensities of this normal mode in SERRS are also enhanced (6.9×10^1).

Consequently, there are two kinds of SERRS in the chemical mechanism for SERRS via the CT from the metal to the molecule at the electronic transitions: (1) the electrons transfer to certain atoms near the metal, and the motions of these atoms along the metal–molecule bonds are involved in the normal modes; and (2) the electrons transfer to certain bonds, and the motions of these bonds along the metal–molecule bonds are predominantly involved in the normal modes. It should be noted that case (2) is less enhanced compared to case (1).

EM enhancement mechanism

From Fig. 3, the excited electron–hole pairs are almost localized on the Au_2 cluster for S_2, which is the intracluster excitation on the resonant transition (the analog to plasmon excitation in large naonoparticles). The intracluster excitation on resonant electronic transition is the visual evidence for the EM enhancement mechanism.

Quantum size effect on the chemical and EM enhancement

As is known, small metal nanoclusters may show remarkable size dependence of absorption and Raman properties,[23] so we study the quantum size effect on the NRS spectrum and mechanism of photoexcitation in absorption.

With the increase in size of the nanoparticle, more electrons (0.148 e) are transferred from the Au_{20} cluster to pyrazine at the ground state (compared to the transferred electrons in pyrazine–Au_2 complex), and so the static permanent polarizability of the pyrazine–Au_{20} complex is much larger than that of the pyrazine–Au_2 complex (Table 1). So, the enhanced intensities of NRS of the pyrazine–Au_{20} complex by static chemical enhancement are much larger than those of the pyrazine–Au_2 complex, which can be seen from Fig. 4. The profile of the NRS spectrum of the pyrazine–Au_{20} complex is similar to that of the pyrazine–Au_2 complex. The four normal modes with high NRS spectral intensities were inserted in Fig. 4, which are the ring stretching mode at 623.7 cm^{-1}, two ring deformation modes at 1019.3 and 1045.9 cm^{-1}, and the ring stretching mode at 1614.0 cm^{-1}.

The lowest 100 singlet excited states of the pyrazine–Au_{20} complex were calculated at the level of TD-B3PW91/LanL2dz (Fig. 5(a)). The first electronic excited state is at 640 nm, and the strongest absorption is in the range 350–400 nm. The SERS spectrum will be a normal Raman spectrum when the energy of the incident light is below 1.937 eV (640 nm), and the enhancement mechanism should be the static chemical enhancement. When the energy of the incident light is above 1.937 eV, then the Raman spectra should be SERRS spectra.

According to the charge difference densities for these electronic excited states (Fig. 5(a)), there are two kinds of electron–hole coherence on electronic excitation. One is the intracluster electron–hole pair excitation, which is the visual evidence for the EM enhancement mechanism of SERRS. The second is the CT from the Au_{20} cluster to pyrazine, which is the visual evidence for chemical enhancement via CT. From Fig. 5(a), in the range 640–525 nm, the SERRS should be contributed from the chemical enhancement via CT from the Au_{20} cluster to pyrazine. In the range 525–400 nm, the SERRS should be contributed from EM enhancement. In the range 400–350 nm, the chemical enhancement via CT is the most important mechanism for SERRS.

Owing to the high computational demands for large clusters (Au_{20}), the quantitative analysis of SERRS was not made in this paper. The qualitative analysis can be referred to the SERRS spectrum in pyrazine–Au_2 for chemical enhancement via CT.

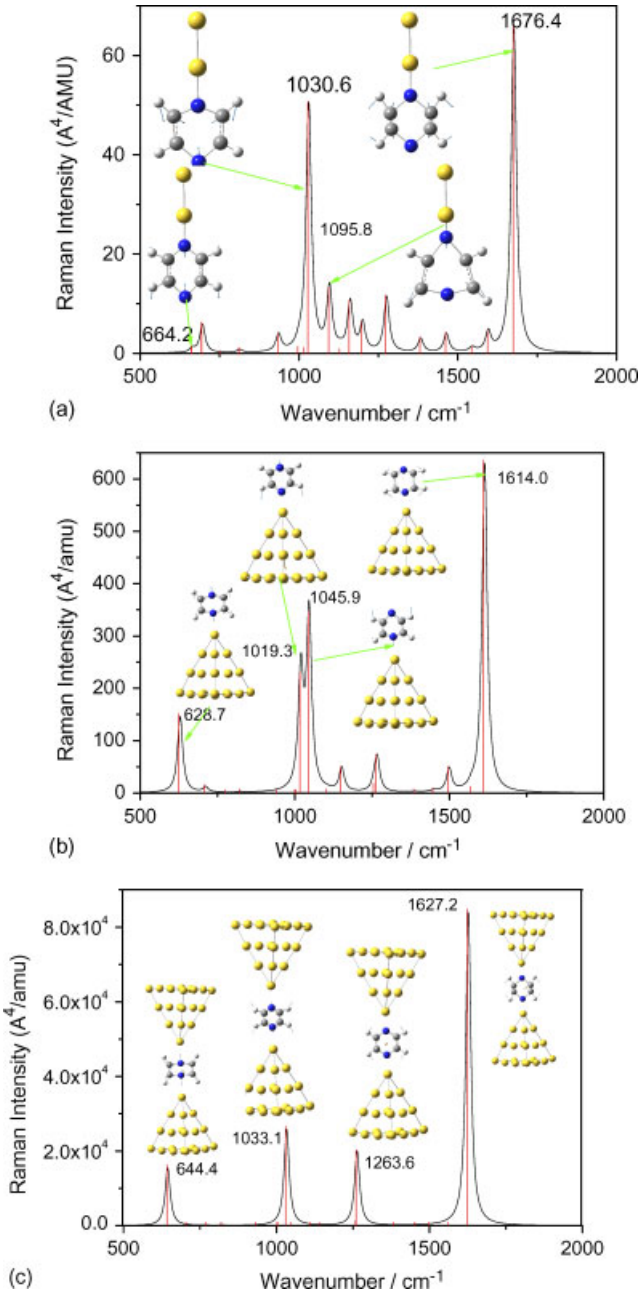

Figure 4. NRS spectra of (a) pyrazine–Au_2 complex, (b) pyrazine–Au_{20} complex, and (c) Au_{20}–pyrazine–Au_{20} junction.

Coupling effect on the chemical and EM enhancement

Owing to the coupling effect of nanoparticles in the Au_{20}–pyrazine–Au_{20} junction, with more electrons (0.25 e) transferring from pyrazine to two Au_{20} clusters, the permanent polarizability of the Au_{20}–pyrazine–Au_{20} junction at the ground state is much larger than that of the pyrazine–Au_{20} complex at the ground state (see data in Table 1), and the static chemical enhancement for the NRS of Au_{20}–pyrazine–Au_{20} junction will be stronger than that of the pyrazine–Au_{20} complex. Comparing their NRS spectra (Fig. 4), one can find that the order of the enhancement is 10^2, due to the coupling effect. The profile of the NRS spectrum of the Au_{20}–pyrazine–Au_{20} junction is similar to that of the pyrazine–Au_{20} complex. The four normal modes with high NRS spectral intensities are shown in Fig. 4, which are the ring stretching mode at 644.4 cm^{-1}, the ring breathing mode at 1033.1 cm^{-1}, the C–H bending mode at 1263.6 cm^{-1}, and the ring stretching mode at 1627.2 cm^{-1}.

Because of the coupling effect of the Au_{20}–pyrazine–Au_{20} junction, the first electronic excited state is red-shifted to 993 nm from 640 nm (compared to pyrazine–Au_{20} complex, Fig. 5(b)), and there are five kinds of electron–hole coherence on the resonant electronic excitations (Fig. 5(b)). The first one (Case A) is CT from two Au_{20} clusters to pyrazine simultaneously; the second (Case B) is CT from one of the Au_{20} clusters to pyrazine; the third (Case C) is tunneling CT (TCT) from one Au_{20} cluster to the other Au_{20} cluster without pyrazine; the fourth (Case D) is the intracluster excitation within one of the Au_{20} clusters; and the last (Case E) is the intracluster excitation within two Au_{20} clusters simultaneously. From Fig. 3(b), the strong peaks in the absorption spectrum belong

Journal of RAMAN SPECTROSCOPY

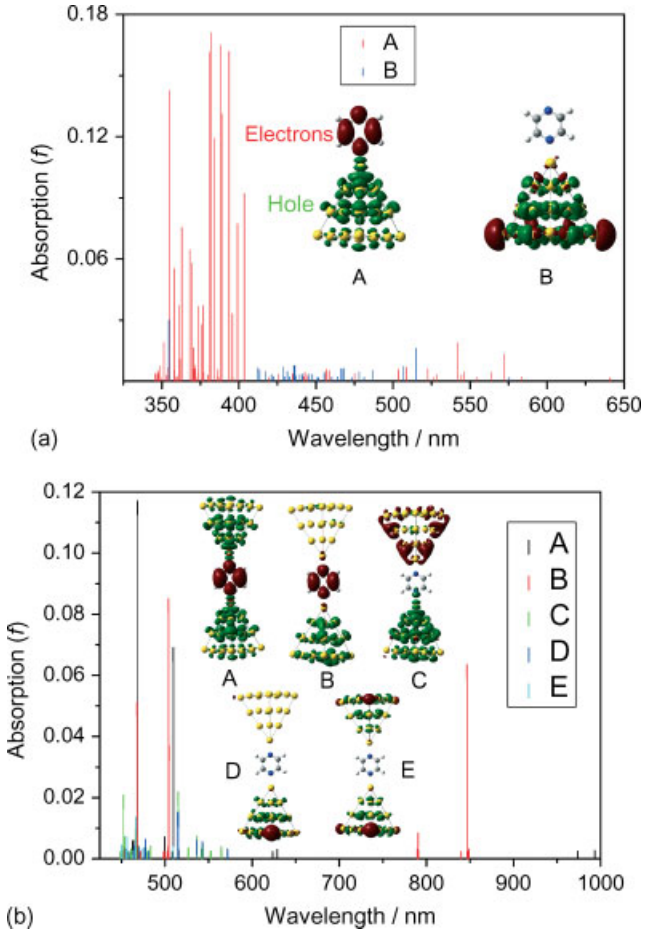

Figure 5. Photoinduced charge transfer in (a) pyrazine–Au_{20} complex, and (b) Au_{20}–pyrazine–Au_{20} junction, where the green and red stand for hole and electron, respectively.

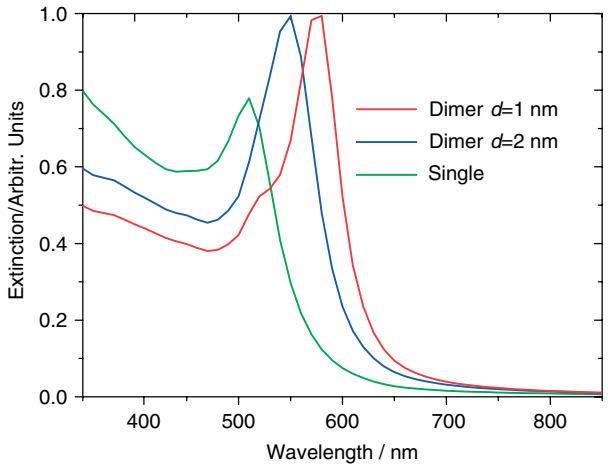

Figure 6. Calculated normalized extinction spectrums of Au nanoparticles. The diameter of the nanoparticle is 50 nm. The separations of the dimer are 1 and 2 nm for the red and blue curves, respectively.

to the first three Cases ((A), (B), and (C)). The first two cases (A) and (B) are the chemical mechanism for SERRS. So the chemical enhancement mechanism should be the dominating mechanism for the SERRS at the Au_{20}–pyrazine–Au_{20} junction. The last two cases (D) and (E) are the EM mechanism for SERRS. The EM 'hot spot' for the junction between small Au_{20} tetrahedral clusters is very weak because of the weak absorption in these regions of optical absorption. The third case (C) should be investigated in detail in future, and more information can be derived from the SERRS spectrum. The junction enhancement effect on the system of pyridine in a metal junction has been pointed out.[24] Owing to high computational demands for large clusters (Au_{20}), a quantitative analysis of SERRS for the coupling effect was not made.

Note that there are two Raman peaks at 1019.3 and 1045.9 cm^{-1} in the pyrazine–Au_{20} complexes, while there is only one peak at 1030.6 cm^{-1} in pyrazine–Au_2 and at 1033.1 cm^{-1} in Au_{20}–pyrazine–Au_{20}. The reason for this is the change of symmetry. Symmeties of isolated pyrazine, pyrazine–Au_2, pyrazine–Au_{20}, and Au_{20}–pyrazine–Au_{20} are D_{2h}, C_{2v}, C_S and C_1, respectively. The C_S symmetry of pyrazine–Au_{20} results in two split deformation modes.[25]

To study the influence of the coupling effect of nanoparticles on the excinction spectra, the normalized extinction spectra of Au nanoparticles were calculated by the general Mie theory,[22] see Fig. 6. The diameter of the nanoparticle is 50 nm. The separations of the dimer are 1 and 2 nm for the red and blue curves, respectively. For a single Au particle, the dipolar resonance peak is at about 510 nm. Owing to the coupling between particles, the resonance peak is red-shifted to 580 nm for the dimer with a separation 1 nm. Mie theory predicted the red shift of the surface Plasmon resonance (SPR) peak from 500 to 580 nm, while from the TD-DFT prediction there exist very weak transitions around 600 nm (Au_{20}–pyrazine–Au_{20}), and the strong absorptions are around 400 and 500 nm for the pyrazine–Au_{20} complex and Au_{20}–pyrazine–Au_{20} junction, respectively. The difference is due to the quantum size effect, since the size of metal in the quantum chemical calculations is several nanometers, while the size (diameter) of metal in the Mie theory is 50 nm.

Conclusion

With charge difference density, visual evidence for chemical and EM enhancement mechanisms of SERRS has been described theoretically and with a unified treatment with quantum theory. The visual CT from the metal to the molecule at the resonant electronic transition is the direct evidence for chemical enhancement. The profile of the preresonant SERRS spectrum at the resonant CT transition further supports our visual evidence. The visual intracluster electron–hole pair excitation at the resonant electronic transition is the direct evidence for EM enhancement. The quantum size effect of the nanoparticle and the coupling effect of the nanoparticles were also investigated. The new mechanism of CT (TCT from one Au_{20} cluster to another) was also visualized with charge difference density.

Acknowledgements

This work was supported by the National Natural Science Foundation of China (Grant Nos: 20703064, 20673012 and 108074234), the National Basic Research Program of China (Grant No: 2009CB930701 and 2007CB936804), the Sino–Swedish collaborations on nanophotonics and nanoelectronics (Grant No: 2006DFB02020), and the 'Bairen' project in CAS.

References

[1] M. Fleischman, P. J. Hendra, A. J. McQuillan, *Chem. Phys. Lett.* **1974**, *26*, 163.
[2] D. L. Jeanmaire, R. P. Van Duyne, *J. Electroanal. Chem.* **1977**, *84*, 1.
[3] M. G. Albrecht, J. A. Creighton, *J. Am. Chem. Soc.* **1977**, *99*, 5215.
[4] M. Moskovits, *Rev. Mod. Phys.* **1985**, *57*, 783.
[5] K. Kneipp, H. Kneipp, I. Itzkan, R. R. Dasari, M. S. Feld, *Chem. Rev.* **1999**, *99*, 2957.
[6] H. X. Xu, E. J. Bjerneld, M. Kall, L. Borjesson, *Phys. Rev. Lett.* **1999**, *83*, 4357.
[7] A. Otto, I. Mrozek, H. Grabhorn, W. Akemann, *J. Phys.: Condens. Matter* **1992**, *4*, 1143.
[8] L. L. Zhao, L. Jensen, G. C. Schatz, *J. Am. Chem. Soc.* **2006**, *128*, 2911.
[9] J. F. Arenas, D. J. Fernández, J. Soto, I. López Tocón, J. C. Otero, J. I. Marcos, *J. Phys. Chem. B* **2003**, *107*, 13143.
[10] J. F. Arenas, J. Soto, J. Lopez-Tocon, D. J. Fernandez, J. C. Otero, J. I. Marcos, *J. Chem. Phys.* **2002**, *116*, 7207.
[11] M. T. Sun, S. B. Wan, Y. J. Liu, J. Yu, H. X. Xu, *J. Raman Spectrosc.* **2008**, *39*, 402.
[12] M. T. Sun, H. X. Xu, *ChemPhysChem* **2009**, *10*, 392.
[13] M. T. Sun, Y. Ding, H. X. Xu, *J. Phys. Chem. B* **2007**, *327*, 111, 13266.
[14] M. T. Sun, S. S. Liu, M. D. Chen, H. X. Xu, *J. Raman Spectrosc.* **2009**, *40*, 137.
[15] M. T. Sun, S. S. Liu, Z. P. Li, J. M. Duan, M. D. Chen, H. X. Xu, *J. Raman Spectrosc.* In press (DOI: 10.1002/jrs.2255).
[16] M. J. Frisch, G. W. Trucks, H. B. Schlegel, G. E. Scuseria, M. A. Robb, J. R. Cheeseman, J. A. Montgomery Jr, T. Vreven, K. N. Kudin, J. C. Burant, J. M. Millam, S. S. Iyengar, J. Tomasi, V. Barone, B. Mennucci, M. Cossi, G. Scalmani, N. Rega, G. A. Petersson, H. Nakatsuji, M. Hada, M. Ehara, K. Toyota, R. Fukuda, J. Hasegawa, M. Ishida, T. Nakajima, Y. Honda, O. Kitao, H. Nakai, M. Klene, X. Li, J. E. Knox, H. P. Hratchian, J. B. Cross, C. Adamo, J. Jaramillo, R. Gomperts, R. E. Stratmann, O. Yazyev, A. J. Austin, R. Cammi, C. Pomelli, J. W. Ochterski, P. Y. Ayala, K. Morokuma, G. A. Voth, P. Salvador, J. J. Dannenberg, V. G. Zakrzewski, S. Dapprich, A. D. Daniels, M. C. Strain, O. Farkas, D. K. Malick, A. D. Rabuck, K. Raghavachari, J. B. Foresman, J. V. Ortiz, Q. Cui, A. G. Baboul, S. Clifford, J. Cioslowski, B. B. Stefanov, G. Liu, A. Liashenko, P. Piskorz, I. Komaromi, R. L. Martin, D. J. Fox, T. Keith, M. A. Al-Laham, C. Y. Peng, A. Nanayakkara, M. Challacombe, P. M. W. Gill, B. Johnson, W. Chen, M. W. Wong, C. Gonzalez, J. A. Pople, *Gaussian 03, Revision E.01*, Gaussian, Inc.: Pittsburgh, PA, **2003**.
[17] P. Hohenberg, W. Kohn, *Phys. Rev.* **1964**, *136*, B864.
[18] J. P. Perdew, K. Burke, Y. Wang, *Phys. Rev. B* **1996**, *54*, 16533.
[19] E. K. U. Gross, W. Kohn, *Phys. Rev. Lett.* **1985**, *55*, 2850.
[20] L. Peyser-Capadona, J. Zheng, J. L. Gonzalez, T. H. Lee, S. A. Patel, R. M. Dickson, *Phys. Rev. Lett.* **2005**, *94*, 058301.
[21] P. J. Hay, W. R. Wadt, *J. Chem. Phys.* **1985**, *82*, 270.
[22] H. X. Xu, *Phys. Lett. A* **2003**, *312*, 411.
[23] L. Jensen, L. L. Zhao, G. C. Schatz, *J. Phys. Chem. C* **2007**, *111*, 4756.
[24] Z. Q. Tian, *J. Raman Spectrosc.* **2005**, *36*, 466.
[25] L. L. Zhao, L. Jensen, G. C. Schatz, *Nano Lett.* **2006**, *6*, 1229.